Journal of Materials Chemistry C

Accepted Manuscript

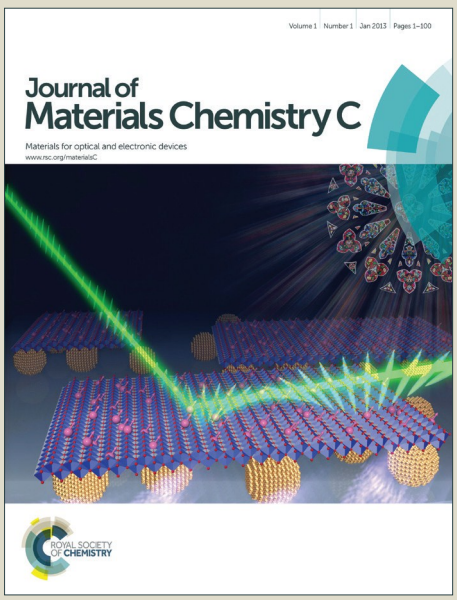

This is an *Accepted Manuscript*, which has been through the Royal Society of Chemistry peer review process and has been accepted for publication.

Accepted Manuscripts are published online shortly after acceptance, before technical editing, formatting and proof reading. Using this free service, authors can make their results available to the community, in citable form, before we publish the edited article. We will replace this *Accepted Manuscript* with the edited and formatted *Advance Article* as soon as it is available.

You can find more information about *Accepted Manuscripts* in the Information for Authors.

Please note that technical editing may introduce minor changes to the text and/or graphics, which may alter content. The journal's standard Terms & Conditions and the Ethical guidelines still apply. In no event shall the Royal Society of Chemistry be held responsible for any errors or omissions in this *Accepted Manuscript* or any consequences arising from the use of any information it contains.

ROYAL SOCIETY OF CHEMISTRY

www.rsc.org/materialsC

Journal of Materials Chemistry C

RSCPublishing

ARTICLE

Multifunctional Polypyrene/Silica Hybrid Coatings with Stable Excimer Fluorescence and Robust Superhydrophobicity Derived from Electrodeposited Polypyrene Films

Cite this: DOI: 10.1039/xoxxoooooox

Received ooth January 2014,
Accepted ooth January 2014

DOI: 10.1039/xoxxoooooox

www.rsc.org/

Lianyi Xu,[a] Faqin Tong,[a] Xuemin Lu,[a] Kai Lu[b] and Qinghua Lu*[a]

A fluorescent and robust superhydrophobic coating based on a fluorinated polypyrene/silica hybrid (FPSH) film was reported. This hybrid film is composed of an underlying polypyrene film and overlying silica layers. The polypyrene film is electrodeposited on an indium tin oxide glass electrode by cyclic voltammetry to provide a petal-like hierarchical rough structure and strong fluorescence with one-step electrochemical polymerization. Notably, the fluorescence emission of this polypyrene film derives from the excimer forms, here reported for the first time. The silica layers are fabricated by a two-step chemical vapor deposition to obtain a supporting silica backbone and low-energy surface. Several critical tests were performed on the FPSH films, confirming that the film is not only a thermally stable, anti-acid/alkali, and anti-impact self-cleaning surface, but also presents a strong green fluorescent emission.

Introduction

The demand to design and fabricate artificial superhydrophobic surfaces with a high water contact angle (WCA > 150°) and low sliding angle (SA < 10°) is constantly increasing. The natural inspiration to create these type of surfaces derives from the self-cleaning and non-wetting properties of the lotus leaf surface and the legs of the water striders.[1,2] An artificial superhydrophobic surface can be readily created by combining materials with appropriate roughness and low-surface-energy in a Cassie state, where the cavities of the rough structure cannot be infiltrated by water.[3,4] This type of coatings has a wide range of potential applications in many technological and scientific fields, such as self-cleaning coatings,[5] anti-bio-fouling coatings,[6] microfluidics,[7] oil-water separation,[8] and bio-technology.[9] As a result, the multi-functionalization of superhydrophobic coatings has recently received special attention, leading to an intensive development of environmentally responsive self-cleaning surfaces,[10,11] transparent superhydrophobic coatings,[12–14] and other materials. Among the various multi-functional coatings, luminescent self-cleaning coatings have generated particular interest, since Char *et al*. firstly reported the preparation of a fluorescent superhydrophobic surface by layer by layer(L-b-L) deposition using charged block copolymer micelles (BCMs) with hydrophobic QDs or fluorescent dyes within their cores.[15,16] Chen *et al*. developed a QDs-based fluorescent superhydrophobic surface via a facile interfacial self-assembly technique.[16b] These coatings may be useful in many photoelectric, sensing, and optical imaging devices, as well as self-cleaning materials in air.

However, a few studies revealed that the preparation of such fluorescent superhydrophobic surfaces is usually limited to only a few fluorescent materials (such as QDs or fluorescent dyes) and technologies (for example self-assembly),[16] potentially restricting their further development. New technologies and materials are highly required for the simple design and quick fabrication of such a robust fluorescent superhydrophobic coating. Among the various luminescent materials, fluorescent π-conjugated polymers are particularly interesting because of their tunable and stable fluorescence and machinability.[15,17,18] Polypyrene, as a representative of π-conjugated polymers, is an important photoluminescence material with high fluorescence quantum yield.[18–25] Most interestingly, polypyrene film can be easily prepared on electrodes by using one-step electrochemical deposition.[18,24] In our previous work,[18] we found that the electrodeposited polypyrene film usually formed a nano/micro-metric hierarchical rough structure, which is advantageous for the fabrication of a superhydrophobic coating.[26] Thus, the polypyrene film may be a promising candidate for the facile fabrication of fluorescent superhydrophobic coatings.

In this work, we propose a new approach for the preparation of fluorescent robust superhydrophobic coatings based on a fluorinated polypyrene/silica hybrid (FPSH) film (Figure 1). This hybrid film is composed of an underlying polypyrene film and overlying silica layers. The former is electrodeposited on an indium tin oxide (ITO) glass electrode by cyclic voltammetry (CV), providing simultaneously a petal-like hierarchical rough structure and strong fluorescence via one-step electrochemical polymerization (Figure 1a). The silica layers are fabricated by two-step chemical vapor deposition (CVD) on the underlying polypyrene film. Firstly,

Journal of Materials Chemistry C Accepted Manuscript

tetraethoxysilane (TEOS) is deposited to improve the mechanical resistance of the polypyrene film; secondly, a 1H,1H,2H,2H-Perfluorooctyltriethoxysilane (POTS) film provides the low-energy surface. After the deposition, the FPSH film presents not only a thermally stable superhydrophobic surface with acid/alkali and water-droplet impact resistance, but also exhibits strong green fluorescent emission (Figure 1b). In addition, we also reported an interesting change of fluorescent properties from the polypyrene emission in solution to the excimer emission in solid polypyrene films. Notably, the green fluorescence of this polypyrene film derives from the excimer forms, here demonstrated for the first time.

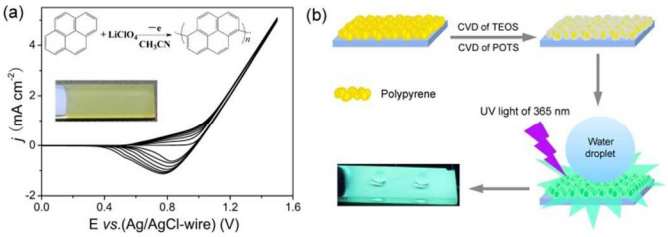

Figure 1. (a) Successive cyclic voltammograms of the electropolymerization of a polypyrene film on the ITO electrode in 0.03 M pyrene/ACN solution containing 0.2 M $LiClO_4$ as a supporting electrolyte; *j* denotes the current density. Insets: Schematic reaction of the electrochemical polymerization of polypyrene (top) and photograph of the resultant polypyrene film on the ITO glass exhibiting a yellow color (bottom). (b) Preparation procedure for fluorescent robust superhydrophobic coatings by using an electrodeposited rough polypyrene film as a photoluminescent material.

Experimental

Materials

Commercial acetonitrile (ACN) in high-performance liquid chromatography grade was provided by Shanghai Lingfeng Chemical Reagent Company and was used without further purification. Pyrene (Adamas, 98%), Tetraethoxysilane (TEOS) (Aladdin, 98%), ammonia solution (Aladdin, 25 ~ 28%), 1H,1H,2H,2H-Perfluorooctyltriethoxysilane (POTS) (Alfa Aesar, 97%), and anhydrous lithium perchlorate ($LiClO_4$) (J&K, 99%) were used directly without further purification.

Characterization

Field emission scanning electron microscopy (FE-SEM) was done by using a Nova NanoSEM instrument (FEI, America). The polymerization degree was determined by Fourier Transform Ion Cyclotron Resonance Mass Spectrometer (FT-ICR MS) (SolariX XR 7.0T, America). The wide angle X-ray diffraction (XRD) pattern was obtained using a D8 ADVANCE X-Ray Polycrystalline Diffractometer (Bruker, Germany). The transmission electron microscopy images and the microscopic electron diffraction (ED) patterns were obtained by using a JEM-2010HT Analytical Transmission Electron Microscope (JEOL, Japan). Static water contact angle measurements were performed using the sessile drop method on a Contact Angle System OCA 20 (DataPhysics Instruments GmbH, Germany) in air. The contact angles reported here were the mean values measured with a 4-μL water droplet at three different positions on each sample. Water sliding angles (SA) were determined by slowly tilting the sample stage until a 4-μL water drop started moving. The adhesion force between the droplet and the sample was assessed by using a high-sensitivity micro-electromechanical balance system (DataPhysics DCAT11, Germany). The sample surface was drawn near and retracted from a 4-μL water droplet suspended on a hydrophobic metal ring at 0.05 mm s^{-1} under ambient conditions (relative humidity of ~ 40%). Chemical compositions of the surfaces were determined by XPS on a Kratos Axis Ultra^{DLD} spectrometer (Kratos Analytical-A Shimadzu, Japan) with monochromatic Al Kα radiation source (1486.6 eV) and takeoff angle of 90°. Fluorescence spectra were detected by using an F-4500 fluorescence spectrophotometer (Hitachi). UV–vis spectra of the films on the ITO substrate were measured on a Perkin-Elmer Lambda 20 UV–vis spectrometer. The photographs and the movies were taken with a camera. The absolute fluorescence quantum yield was measured by using a QuantaMaster 40 with integrating sphere (Photon Technology International Inc.). The in-situ fluorescence intensity under various temperatures was estimated by using QM/TM/IM Steady-State & Time-Resolved Fluorescence Spectrofluorometer (Photon Technology International Inc.). The impact of the water droplet on the coating was captured using a high-speed camera (Motion Studio Cameras SDK, IDT, Inc.). The fluorescence images of FPSH film were captured with inverted fluorescence microscope (IX 71, Olympus) equipped with a CCD camera.

Electrochemical Experiments

All the electrochemical experiments were conducted in an electrochemical cell (1 × 1 × 4.5 cm^3) with a three-electrode system by using a computer-controlled CHI 630E Electrochemical Analyzer. The working electrode was indium tin oxide (ITO) glass (< 10 Ω sq^{-1}, 0.9 × 5 cm^2), successively washed under ultrasonication with deionized water and absolute ethanol, and then dried with a stream of N_2 before use. The counter electrode was platinum wire (1 mm diameter), which was cleaned before each examination. An Ag/AgCl wire was used as a quasi-reference electrode. All electrochemical experiments were performed at room temperature and < 40% relative humidity.

Electrochemical Preparation of Polypyrene Films

Polypyrene films were electrodeposited on ITO electrodes by cyclic voltammetry (CV) between 0 and +1.5 V in 0.03 M pyrene/ACN solution containing 0.2 M $LiClO_4$ as a supporting electrolyte. The thickness of the polypyrene film was tuned by controlling the electrodeposition charge (*Q*) approximately at 150 ± 20 mC cm^{-2}. Before characterization, all films were rinsed with 50% ethanol water (about 1 mL) for two times and then dried at room temperature for several minutes under flowing N_2.

Preparation of the Silica-coated Superhydrophobic Polypyrene Films

To cover the polypyrene films with silica layers, chemical vapor deposition (CVD) of TEOS was performed at room temperature for 30 h, that is, the films were placed in a closed desiccator together with two open vessels containing about 2 mL of TEOS and 1 mL of aqueous ammonia solution, respectively.[5b,12] Silica layers were formed on polypyrene films by hydrolysis and condensation of TEOS catalyzed by

Journal of Materials Chemistry C Accepted Manuscript

This journal is © The Royal Society of Chemistry 2012

ammonia.[5b] The silica-layer-encased polypyrene films retained the petal-like structure. To create superhydrophobic silica coatings, CVD of POTS was performed at room temperature for 12 h in a similar closed desiccator where the silica coatings were placed together with two open vessels containing 0.2 mL of POTS and 0.2 mL of aqueous ammonia solution, respectively.

Preparation of large-scale and flexional FPSH films

The large-scale and flexional FPSH films were prepared on the stainless steel woven wire mesh (100 meshs, 17 × 8 cm^2) and the plastic transparent ITO-PET film (35 ± 5 Ω sq^{-1}, 5 × 3 cm^2). In the three-electrode electrochemical system, the stainless steel woven wire mesh or the plastic transparent ITO-PET film was used as the working electrode, and the stainless steel woven wire mesh electrode with a larger area than that of working electrode was used as counter-electrode. The polypyrene films were electrodeposited by using the constant potential of +1.5 V in 0.03 M pyrene/ACN solution containing 0.2 M $LiClO_4$ as a supporting electrolyte. The thickness of the polypyrene was controlled by using Q = 150 ± 20 mC cm^{-2}. The FPSH films on the stainless steel woven wire mesh and the plastic transparent ITO-PET film were prepared with the same CVD condition demonstrated above.

Results and discussion

Preparation and Morphologies

The FPSH film was created from an electrodeposited polypyrene film. In a three-electrode system, the polypyrene film was electrodeposited on ITO glass by using a CV method in a 0.03 M pyrene/acetonitrile (ACN) solution containing 0.2 M $LiClO_4$ as a supporting electrolyte (inset in Figure 1a). Note that the concentration of the pyrene monomer is limited to 0.03 M, since a higher or lower monomer concentration (such as 0.05 M or 0.01 M) is unfavorable to obtain the required polypyrene film. By controlling the electrodeposited charge (Q) at 150 ± 20 mC cm^{-2}, a uniform yellow polypyrene film can be deposited (see the photograph in the inset of Figure 1a). In general, the morphology or the photoelectric properties of electrodeposited π-conjugated polymer films are affected by the electrode materials, applied potential, electrolyte solution, monomers, and even concentration of the monomers. In our electrochemical experimental system, the resulting polypyrene film presents a petal-like rough morphology, as revealed by the scanning electron microscopy (SEM) images (Figure 2a). The magnified SEM image shows in more detail the micro/nanometer-scale drape structure (Figure 2b). This morphology may be attributed to the particular electrochemical system.[18–25]

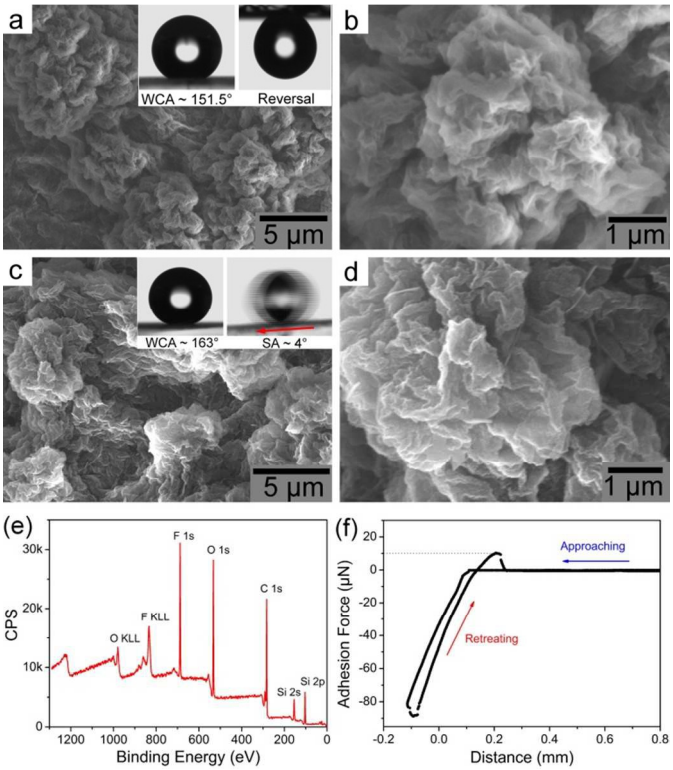

Figure 2. (a) Scanning electron microscopy (SEM) image of the petal-like porous structure of the polypyrene film. Insets: WCA measurement on the film (WCA ca. 151.5° ± 1°) (left); The water droplet (4 μL) did not roll off but remained attached to the surface even when the surface was inverted (right). (b) Magnified image of the polypyrene film. (c) SEM image of the resulting petal-like porous FPSH film after CVD of TEOS and fluorination. Insets: the resultant FPSH film had a static WCA of 163° ± 1° (left) and the water droplet on a 4° tilted FPSH film lost adhesion and rolled off. (d) Magnified image of the resulting FPSH film. (e) X-ray photoelectr on spectroscopy of the FPSH film. (f) Force–distance curves recorded for a water droplet (4 μL) gradually approaching and retreating from the FPSH film surface.

The polymerization degree of the electrodeposited polypyrene was estimated about 6 ~ 11 pyrene units, which means that the resulting polypyrene is only an oligomer (screenshots in Figure S1). This kind of oligopyrene film may be fragile and easy to damage under an external impact force because of its rigid pyrene ring structure.[22,24] To protect the peculiar roughness morphology and improve the impact resistance, we tried to cover the resulting polypyrene film with a silica layer. For this purpose, TEOS catalyzed by ammonia was deposited via CVD in a closed container at room temperature.[5b,12] After 30 h, a hydrophilic polypyrene/silica hybrid coating was formed. To reduce its surface energy, another CVD of POTS was further performed in a similar closed container at room temperature for 12 h. After this step, the FPSH film was ready. We found that the FPSH film perfectly inherited the petal-like rough morphology of the polypyrene film (Figure 2c). The thickness of FPSH film was estimated to be approximately 10 μm (Figure S2). Furthermore, the magnified SEM image of the FPSH film still shows the micro/nanometer-scale drape structure, although the silica layer with the thickness of ca. 30 ~ 40 nm was deposited on the underlying polypyrene film (Figure 2d and Figure S3).

Journal of Materials Chemistry C Accepted Manuscript

Superhydrophobicity and Self-cleaning Properties

A superhydrophobic surface with a water contact angle > 150° may be either a water super-adhesion surface or a water self-cleaning surface, depending on the rough structure of the surface and the surface energy. The details of the wetting properties can be confirmed by examining the water sliding angle. The as-prepared FPSH film has a high water contact angle of 163° ± 1° and a small sliding angle of about 4° ± 1° (inset in Figure 2c), indicating that the FPSH film is an anti-adhesive coating with self-cleaning ability (Movie S1). Owing to the so-called Cassie surface state, water droplets placed on such coatings sit on top of air cushions trapped beneath the droplets.[3] Conversely, the pure polypyrene film, before the double CVD process, presented a super adhesive surface with a WCA of 151.5° ± 1° and a big sliding angle > 90° even when reversed (Wenzel adhesion state; inset in Figure 2a).[11] This wetting transition from Wenzel to Cassie states can be attributed mainly to the successful introduction of low surface energy fluorosilane on the petal-like rough structure, as evidenced by the strong F1s peak at 691.8 eV in the X-ray photoelectron spectroscopy (XPS) measurement (Figure 2e). The adhesion force between the water and the FPSH film surface was also estimated by detecting the force–distance curves of a water droplet (4 μL) moved near to and far from the film surface (Figure 2f). The measured adhesion force was only about 10.2 μN. This very weak adhesion force could not prevent water droplets (4 μL) from rolling away from the FPSH film surface.

Optical Properties and Photoluminescence

Figure 3a and b show the excitation and fluorescent emission spectra of the FPSH film, polypyrene film and its dimethyl formamide (DMF) solution (their UV/vis spectra are shown in Figure S4). The polypyrene film showed a strong emission peak centered at 498.5 nm (Figure 3a (red)), when excited at 408 nm (the inset of Figure 3a (black)), and the film emitted a bright blue-green fluorescence when exposed to 365 nm UV light, demonstrating its good fluorescent property (Figure 3c (left)). Notably, the polypyrene dissolved in DMF exhibited a different emission peak centered at 451.5 nm (Figure 3b (blue)) when excited at 349 nm (Figure 3b (black)), while the emission peak centered at 498.5 nm presented in the fluorescent spectrum of solid polypyrene disappeared completely. Furthermore, the polypyrene in DMF emitted a bright blue fluorescence (under 365 nm UV light) (Figure 3c (right)). Obviously, the fluorescence properties of the polypyrene undergo a significant change when passing from solution to solid state, and a significant red-shift of about 47 nm in their fluorescent spectra can be detected. In general, the excimer emission bands of pyrene species are located above 460 nm.[27] The fluorescent emission centered at 498.5 nm may originate from the excimer forms in the solid polypyrene film.[21,22,27] Furthermore, such an excimer emission can be readily realized when the electrodeposition charge is more than 105.3 mC cm^{-2} (Figure S5 and S6)

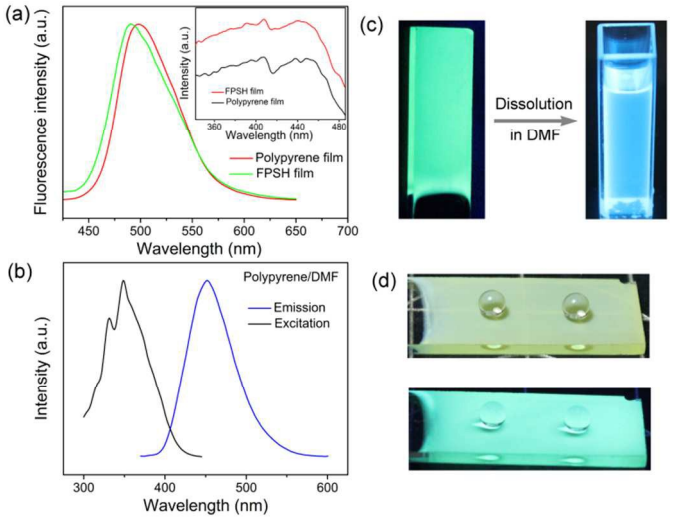

Figure 3. (a) Fluorescence emission spectra of the polypyrene film (λ_{ex} = 408 nm, red) and FPSH film (λ_{ex} = 408 nm, green). Inset: the excitation spectra of the polypyrene (λ_{em} = 498.5 nm, black) and FPSH (λ_{em} = 490.5 nm) films. (b) Excitation (λ_{em} = 451.5 nm, black) and fluorescence emission spectra (λ_{ex} = 349 nm, blue) of polypyrene dissolved in DMF. (c) Fluorescence photograph of the polypyrene film (blue-green fluorescence, left) and polypyrene dissolved in DMF (blue fluorescence, right), under 365 nm UV light. (d) Photograph of randomly distributed water droplets (8 μL) on the yellow FPSH film (top). These water droplets show nearly spherical shape. Under 365 nm UV light, the FPSH film emits strong blue-green fluorescence light (bottom), and the water droplets still retain their spherical shape.

The strong excimer emission in a polypyrene film is a unique phenomenon. During the electrochemical process, the oligopyrenes were gradually deposited on the electrode. The oligomer aggregation with intermolecular overlapping pyrene units may result in intermolecular π–π* stacking interactions[27] forming the excimer in the solid polypyrene film. The X-ray diffraction (XRD) pattern of the polypyrene film presents a very broad diffraction peak (centered at 2θ = 23.5°) that might originate from stacked pyrene units.[27d] Furthermore, a good progression of diffraction peaks at 2θ angles of 5.7°, 11.4°, and 16.6° confirms that the oligopyrene film also contains several microcrystalline structures (see supporting information section and Figure S7a (bottom)).[21,22,27] In addition, the micro/nanometer-scale porous drape structure of the polypyrene film facilitates the reduction of the fluorescence quenching.[27] These unique structural characteristics may lead to a strong excimer emission in solid polypyrene films.

After depositing the silica layer, the resulting FPSH film perfectly inherited the fluorescence properties of the polypyrene film. A strong fluorescence emission centered at 490.5 nm (Figure 3a (green)) upon excitation at 408 nm (the inset of Figure 3a (red)) was readily detected. A slight blue-shift of about 8 nm was observed, probably due to the fact that the incorporation of silica layer into the aggregate oligopyrene leads to an alteration of the micro-environment around the oligopyrene excimers, involving intermolecular distance and pressure.[21,22,27] Notably, the shape and the maximum position of the excimer emission band of the FPSH film were not obviously affected by the excitation wavelengths from 350 to 490 nm (Figure S8 and S9). This means that the fluorescent emission spectra of the FPSH film are significantly different

Journal of Materials Chemistry C Accepted Manuscript

This journal is © The Royal Society of Chemistry 2012

from that of polypyrene/DMF solution, even if exciting them with the same excitation wavelength, such as 350 and 408 nm. Nevertheless, the FPSH film has an absolute fluorescence quantum yield of about 9.1% (excitation at 408 nm) (Figure S10). Figure 3(d) shows the original and fluorescent photographs of the superhydrophobic FPSH coating. Water droplets (8 μL) placed on such a luminous FPSH film surface (under 365 nm light) clearly exhibits a nearly spherical shape. Therefore, the FPSH film not only has good superhydrophobic self-cleaning properties, but also presents excellent fluorescent characteristics.

Robust fluorescence and superhydrophobicity

The stability of FPSH films at high temperature was investigated to support their practical application. As shown in Figure 4a, the fluorescence intensity of the coating only slightly decreases with increasing the temperature from 10 °C to 90 °C. Nevertheless, the WCA and SA of the film remained almost unchanged, even after annealing the sample at temperatures up to 200 °C for 1 h in air (Figure 4b). Interestingly, the FPSH film still exhibited strong fluorescence after annealing at 200 °C (inset in Figure 4b (left)). These results indicate that the FPSH film possesses an excellent thermal stability. The FPSH film also exhibits a strong repellence to water (WCA > 150°) for an acid or a base droplet, as evidenced by measuring the CA and SA of the water droplets with pH values of about 1 and 13 (Figure 4b and its inset (right)).

In many practical applications, superhydrophobic coatings often suffer from a water-droplet impact during which a wetting pressure ($P_{wetting}$) is generated. At that time, the change of wetting state of the rough surface depends on the balance between the $P_{wetting}$ and the capillary pressure ($P_{capillary}$) generated within the surface texture.[28,29] If $P_{wetting}$ is > $P_{capillary}$, it leads to the water-droplet wetting the coating surface. Thus, for practical applications, the investigation of water-droplet impingement on superhydrophobic surfaces has recently received increasing attention.[28,29] In our work, water-droplet impact experiments were performed. Water droplets (20 μL, radius of about 1.68 mm) were used to impact the FPSH film at the velocity (V_0) of 1.08 m s^{-1} (fall height of 6 cm). The impingement process of water droplets on the surface was captured by a high-speed camera (Figure 4c). The third image in Figure 4c shows that a large round hat with an undulated rim was formed on the FPSH film surface at the moment of the high-velocity impact; after that, the water droplet rebounded without any pinned satellite droplet leaving the surface. This result indicates that the coating showed the robust superhydrophobicity during the impact of water droplets. In fact, during the water-droplet impact, the wetting pressure $P_{wetting}$ comprises two components: the water hammer pressure (P_{WH}) at the contact stage and the incompressible dynamic pressure (P_D) at the spreading stage of the impingement.[29] At the contact stage, the initial impact on the rough surface generates a P_{WH} resulting from the compression of the water droplet behind the shock wave envelope. The water hammer pressure can be estimated as:[29]

$$P_{WH} \approx 0.2\rho C V_0 \quad (1)$$

where C is the sound velocity in water. In our work, the water impact generated a P_{WH} of about 0.32 MPa on the rough surface. At the spreading stage, the pressure rapidly reduces to P_D while the droplet contact line expands. The P_D can be provided by the equation[29]

$$P_D = 0.5\rho V_0^2 \quad (2)$$

estimated to be only ca. 0.58 kPa. Although the water-air interfaces below the compressed region suffered a push with a maximum pressure of ca. 0.32 MPa, the FPSH film still kept its non-adhesive superhydrophobic properties. Its robust superhydrophobicity could be attributed to its high $P_{capillary}$ (>>$P_{wetting}$) generated within its petal-like hierarchical rough structure. Even after impacting with a series of water droplets (radius of 2.1 mm) from a height of 6 cm at a dropping rate of one droplet per second for more than 12 h, the FPSH film still retained its superhydrophobicity with a WCA of about 153.9° ± 1° (Figure S11). Such superhydrophobic FPSH film could also be used under water where the film still presented the anti-wettability with strong fluorescence (Figure S12).

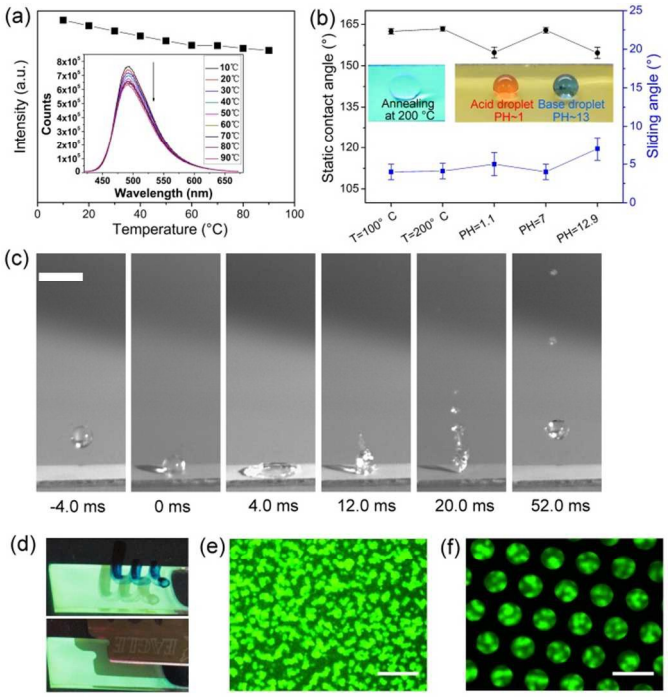

Figure 4. (a) Fluorescent intensity of the FPSH film at different temperatures ranging from 10 to 90 °C (λ_{ex} = 408 nm). Inset: corresponding emission spectra. (b) Anti-wetting stability of FPSH film evaluated by measuring the WCA and SA after annealing at 100 and 200 °C for 1 h in air, and measuring the CA and SA of water droplets with pH 1and 13. Insets: fluorescent photograph of the film after annealing at 200 °C (left), and photograph of the film with an acid droplet (red, 8 μL H_2SO_4 solution of methyl orange with pH ~ 1) and a base droplet (blue, 8 μL NaOH solution of thymolphthalein with pH ~ 13) (right). (c) Sequential photographies of a 20-μL water droplet bouncing off the FPSH film at an impact velocity of 1.08 m s^{-1}. The scale bar is 4 mm. (d) Photographies of the letters and blade casting their shadows onto the films. (e) The fluorescent microscope picture of the FPSH film excited by the blue light. The scale bar is 100 μm. (f) The fluorescent microscope pictuere of the FPSH film covered with a micro grid. The scale bar is 100 μm.

In order to investigate the possible application in the display devices, we also evaluated the ability to display patterns on this fluorescent film when exposed on the 365 nm UV light. As shown in Figure 4d, the letters (top) and the blade (bottom) can cast their shadows onto the films at a height of about 4.4 mm, leaving their special shades with the clear boundaries. This

Journal of Materials Chemistry C Accepted Manuscript

result indicated that the resulting FPSH film is a uniform fluorescent coating. The fluorescent microscope picture of the FPSH film excited by the blue light exhibited cleanly many small green luminous protuberances on the fluorescent film (Figure 4e). When a micro grid with the bore diameter of about 60 μm was covered on the FPSH film, the fluorescence array pattern at micrometer scale could be also created (Figure 4f).

Large-scale and flexional fluorescent superhydrophobic film

Electrochemical deposition technique provides a facile and controllable way to prepare rapidly the large-area π-conjugated polymer films on the various conducting substrates, including stainless steel sheets, stainless steel woven wire mesh, titanium sheets, Ag sheets and plastic transparent ITO-PET film. In this work, for further investigating the potential applications of the FPSH film, such as in display devices or luminous signs, the large-scale and flexional FPSH films were prepared by electrodepositing polypyrene on a conducting stainless steel woven wire mesh and a plastic transparent ITO-PET film (Figure 5). As shown in Figure 5a, the yellow FPSH film can adhere well to the large stainless steel woven wire mesh. The FPSH-enclosing stainless steel woven wire mesh presents a superhydrophobicity with 4-μL WCA of 162° ± 1° (inset of Figure 5a), and the water droplets (20 ~ 30 μL) dripping on such surface do not be stuck but roll off rapidly, indicating the self-cleaning property (Movie S2 and S3). When exposed to 365 nm UV light, the FPSH-enclosing stainless steel woven wire mesh emitted a bright blue-green fluorescence at large scale, indicating its good fluorescent property (Figure 5b). The meshy fluorescent patterns also can be observed cleanly in its fluorescent microscope picture excited by the blue light, further indicating the FPSH film enclosed the stainless steel woven wire mesh very well (inset of Figure 5b). Interestingly, although the fluorescent polypyrene moieties in FPSH film were separated from the species in aqueous solution by the superhydrophobic surface, the low-cost FPSH-enclosing stainless steel woven wire mesh can also be used as chemical sensor in the low-surface-energy organic solution (such as the 4-nitrobenzene chloride in ethanol solution) (Figure S13 and S14)

Similarly, the FPSH-coating plastic transparent ITO-PET film also exhibits the large-scale and flexional fluorescent superhydrophobicity, as evidenced by its curved luminescence surface excited at 365 nm and its high WCA of about 160.5° ± 1° (Figure 5c and d, Figure S15 and Movie S4). These large-scale and flexional fluorescent superhydrophobic film prepared by electrochemical strategy may be have a good use in many practical applications.

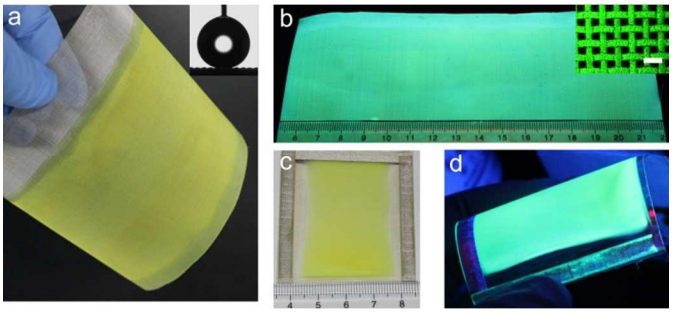

Figure 5. (a) The FPSH film can be prepared easily on the large-scale and flexional stainless steel woven wire mesh (100 mesh). Inset: the WCA measurement on FPSH-enclosing stainless steel woven wire mesh (WCA ca. 162° ± 1°). (b) The FPSH film on the stainless steel woven wire mesh emitted the blue-green fluorescence under UV of 365 nm. Inset: The fluorescent microscope picture of the stainless steel woven wire mesh enclosed by the fluorescent FPSH film excited by the blue light. The scale bar is 200 μm. (c) The FPSH film prepared on the plastic transparent ITO-PET film substrate. (d) The curved fluorescent FPSH film on the ITO-PET substrate under UV of 365 nm.

Conclusions

In conclusion, we developed a fluorescent and superhydrophobic self-cleaning coating based on a fluorinated electrodeposited-polypyrene/silica hybrid film. The electrodeposited polypyrene film has a petal-like porous structure and strong fluorescence, which is advantageous for the fabrication of superhydrophobic coatings with fluorescence properties. To protect the fragile structure of the polypyrene film and improve its water-impact resistance, we coated the film with a silica layer made via CVD. After fluorination, the as-prepared FPSH film not only exhibited a superhydrophobic self-cleaning surface with a static water contact angle of 163° ± 1° and a sliding angle of 4° ± 1°, but also ideally inherited the excellent blue-green fluorescence of the polypyrene film. The fluorescence can be attributed to the excimer emission in the polypyrene film. This fluorescent superhydrophobic bifunctional coating was found to be able to withstand harsh environmental tests. After high-temperature annealing, up to 200 °C for 1 h in air, its superhydrophobicity and fluorescence remained almost unchanged. The coating also showed a strong repellence to acid or base droplets, and a strong water droplet impact resistance. Furthermore, such FPSH film also can be prepared readily on the large-scale and flexional conducting substrates, such as the steel woven wire mesh and plastic transparent ITO-PET film. The fluorescent and robust superhydrophobic self-cleaning coatings would have potential application in photoluminescence windows, sensors, external sign coatings, and so on.

Acknowledgments

This work was supported by 973 Projects (2012CB933803, 2014CB643605), the National Science Fund for Distinguished Young Scholars (50925310), the National Science Foundation of China (21374060, 51173103), and Excellent Academic Leaders of Shanghai (11XD1403000).

Notes and references

[a] School of Chemistry and Chemical Engineering, State Key Laboratory of Metal Matrix Composite, Shanghai Jiao Tong University, 800 Dongchuan Road, Shanghai, 200240, People's Republic of China
E-mail: qhlu@sjtu.edu.cn.
[b] Southwest Weiyu Middle School VIA, 671 Yishan Road, Shanghai, 200030, People's Republic of China

Electronic Supplementary Information (ESI) available: [Polymerization degree, Cross-sectional SEM image of the film, Silica layer thickness, Microcrystalline oligopyrene, Absolute fluorescence quantum yield, Hydraulic Pressure Resistance]. See DOI: 10.1039/b000000x/

Journal of Materials Chemistry C Accepted Manuscript

This journal is © The Royal Society of Chemistry 2012

1 a) K. S. Liu and L. Jiang, *Annu. Rev. Mater. Res*., 2012, **42**, 231; b) M. J. Liu, Y. M. Zheng, J. Zhai and L. Jiang, *Acc. Chem. Res*., 2010, **43**, 368; c) W. Barthlott and C. Neinhuis, *Planta*, 1997, **202**, 1; d) T. Darmanin, E. T. de Givenchy, S. Amigoni and F. Guittard, *Adv. Mater*., 2013, **25**, 1378.

2 a) Y. Li, L. Li and J.Q. Sun, *Angew. Chem.*, 2010, **122**, 6265; b) H. Zhou, H. X. Wang, H. T. Niu, A. Gestos, X. G. Wang and T. Lin, *Adv. Mater*., 2012, **24**, 2409; c) Q. Y. Liu, L. Gao and L. Jiang, *Prog. Nat. Sci.: Mater. Int.*, 2013, **23**, 532.

3 a) A. B. D. Cassie and S. Baxter, *Trans. Faraday Soc*., 1944, **40**, 546; b) A. Lafuma and D. Quéré, *Nat. Mater*., 2003, **2**, 457; c) A. Tuteja, W. Choi, M. Ma, J. M. Mabry, S. A. Mazzella, G. C. Rutledge, G. H. McKinley and R. E. Cohen, *Science*, 2007, **318**, 1618.

4 K. -Y. Yeh and L. -J. Chen, *Langmuir*, 2008, **24**, 245.

5 a) S. T. Yohe, Y. L. Colson and M. W. Grinstaff, *J. Am. Chem. Soc*., 2012, **134**, 2016–2019; b) X. Deng, L. Mammen, H. J. Butt and D. Vollmer, *Science*, 2012, **335**, 67; c) Z. P. Wu, Q. F. Xu, J. N. Wang and J. Ma, *J. Mater. Sci. Technol.*, 2010, **26**, 20; d) T. Verho, C. Bower, P. Andrew, S. Franssila, O. Ikkala and R. H. A. Ras, *Adv. Mater.*, 2011, **23**, 673; e) P. A. Levkin, F. Svec and J. M. J. Fréchet, *Adv. Funct. Mater*., 2009, **19**, 1993.

6 C. M. Kirschner and A. B. Brennan, *Annu. Rev. Mater. Res.*, 2012, **42**, 211.

7 a) D. L. Tian, J. Zhai, Y. L. Song and L. Jiang, *Adv. Funct. Mater.*, 2011, **21**, 4519; b) H. Mertaniemi, V. Jokinen, L. Sainiemi, S. Franssila, A. Marmur, O. Ikkala and R. H. A. Ras, *Adv. Mater.*, 2011, **23**, 2911.

8 a) Y. Yu, H. Chen, Y. Liu, V. Craig, L. H. Li and Y. Chen, *Adv. Mater. Interfaces*, 2014, 10.1002/admi.201300002; b) X. Gao, L.-P. Xu, Z. Xue, L. Feng, J. Peng, Y. Wen, S. Wang and X. Zhang, *Adv. Mater.*, 2014, **26**, 1771.

9 E. Ueda and P. A. Levkin, *Adv. Mater*., 2013, **25**, 1234.

10 a) L. Y. Xu, X. M. Lu, M. Li and Q. H. Lu, *Adv. Mater. Interfaces*, 2014, 10.1002/admi.201400011; b) M. J. Cheng, Q. Liu, G. N. Ju, Y. J. Zhang, L. Jiang and F. Shi, *Adv. Mater.*, 2014, **26**, 306.

11 a) Y. K. Lai, F. Pan, C. Xu, H. Fuchs and L. F. Chi, *Adv. Mater*., 2013, **25,** 1682; b) Y. K. Lai, X. F. Gao, H. F. Zhuang, J. Y. Huang, C. J. Lin and L. Jiang, *Adv. Mater*., 2009, **21**, 3799.

12 X. Deng, L. Mammen, Y. F. Zhao, P. Lellig, K. Müllen, C. Li, H. J. Butt and D. Vollmer, *Adv. Mater.*, 2011, **23**, 2962.

13 K. C. Park, H. J. Choi, C. H. Chang, R. E. Cohen, G. H. McKinley and G. Barbastathis, *ACS Nano*, 2012, **6**, 3789.

14 Y. Gahmawan, L. Xu and S. Yang, *J. Mater. Chem. A*, 2013, **1**, 2955.

15 a) S. -Y. Ju, W. P. Kopcha and F. Papadimitrakopoulos, Science, 2009, **323**, 1319; b) C. Minard-Basquin, T. Weil, A. Hohner, J. O. Rädler and K. Müllen, *J. Am. Chem. Soc*,. 2003, 125, 5832; c) W. J. Hong, Y. X. Xu, G. W. Lu, C. Li and G. Q. Shi, *Electrochem. Commun.*, 2008, **10**, 1555.

16 a) J. Hong, W. K. Bae, H. Lee, S. Oh, K. Char, F. Caruso and J. Cho, *Adv. Mater*,. 2007, **19**, 4364; b) L. R. Hou, C. F. Wang, L. Chen and S. Chen, *J. Mater. Chem.*, 2010, **20**, 3863; c) S. Y. Yang, L. F. Wang, C. -F. Wang, L. Chen and S. Chen, *Langmuir*, 2010, **26**, 18454; d) S. Y. Yang, C. Zhou, J. B. Liu, M. X. Yu and J. Zheng, *Adv. Mater.*, 2012, **24**, 3218.

17 a) D. Dudenko, A. Kiersnowski, J. Shu, W. Pisula, D. Sebastiani, H. W. Spiess and M. R. Hansen, *Angew. Chem. Int. Ed.*, 2012, **51**, 11068; b) M. T. Dang, L. Hirsch, G. Wantz and J. D. Wuest, *Chem. Rev*., 2013, **113**, 3734.

18 L. Y. Xu, J. S. Zhao, R. M. Liu, H. T. Liu, J. F. Liu and H. S. Wang, *Electrochim. Acta*, 2010, **55**, 8855.

19 C. Zhang, Y. Xu, N. Wang, Y. Xu, W. Xiang, M. Ouyang and C. Ma, *Electrochim. Acta*, 2009, **55,** 13.

20 Z. J. Zhao, X. J. Xu, F. Wang, G. Yu, P. Lu, Y. Q. Liu and D. B. Zhu, *Synthetic Met.*, 2006, **156**, 209.

21 Y. Q. Chen, H. Bai, Q. Chen, C. Li and G. Q. Shi, *Sensor. Actuat. B-Chem,* 2009, **138**, 563.

22 L. T. Qu and G. Q. Shi, *Chem. Commun.*, 2004, 2800.

23 B. Y. Lu, J. K. Xu, C. L. Fan, F. X. Jiang and H. M. Miao, *Electrochim. Acta*, 2008, **54**, 334.

24 G. W. Lu and G. Q. Shi, *J. Electroanal. Chem.*, 2006, **586**, 154.

25 G. Zotti and G. Schiavon, Synth. Met., 1992, **47**, 193.

26 a) E. L. Foster, A. C. C. De Leon, J. Mangadlao and R. Advincula, *J. Mater. Chem*., 2012, **22**, 11025; b) L. B. Xu, Z. W. Chen, W. Chen, A. Mulchandani and Y. S. Yan, *Macromol. Rapid Commun*., 2008, **29**, 832; c) T. Darmanin and F. Guittard, *J. Am. Chem. Soc*., 2011, **133**, 15627; d) T. Darmanin, E. T. de Givenchy, S. Amigoni and F. Guittard, *Adv. Mater*., 2013, **25**, 1378.

27 a) F. M. Winnik, *Chem. Rev*., 1993, **93**, 587; b) H. Ringsdorf and J. Venzmer, *Macromolecules*, 1991, **24**, 1678; c) T. Förster, *Angew. Chem. Int. Ed. Engl.*, 1969, **8**, 333; d) W. Cho, H. J. Lee, G. Choi, S. Choi and M. Oh, *J. Am. Chem. Soc.*, 2014, **136**, 12201.

28 T. Deng, K. K. Varanasi, M. Hsu, N. Bhate, C. Keimel, J.Stein and M. Blohm, *Appl. Phys. Lett.*, 2009, **94**, 133109.

29 A. Checco, A. Rahman and C. T. Black, *Adv. Mater.*, 2014, **26**, 886.

Journal of Materials Chemistry C Accepted Manuscript

A fluorescent and robust superhydrophobic coating based on a fluorinated polypyrene/silica hybrid film was prepared readily on the large-scale substrates.

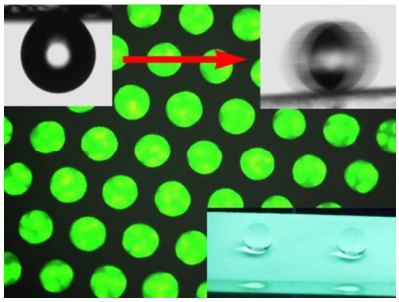

Journal of Materials Chemistry C Accepted Manuscript